nature physics

Article

https://doi.org/10.1038/s41567-023-02127-y

High-harmonic generation driven by quantum light

In the format provided by the authors and unedited

Supplementary Information: High harmonic generation driven by quantum light

Alexey Gorlach†, Matan Even Tzur†, Michael Birk, Michael Krüger,

Nicholas Rivera, Oren Cohen and Ido Kaminer

This supplementary information file contains additional details about the analytical and numerical results presented in the main text. In Section I, we develop a general theory of high harmonic generation (HHG) driven by light with arbitrary photon statistics. In Section II, we derive the cutoff laws presented in the main text. In Section III, we provide the details of the numerical calculation of the HHG spectrum. In Section IV, we show that the threshold of intensity sufficient for the generation of HHG is lower by an order of magnitude for a BSV drive, compared to a coherent state drive.

I. General formalism of light emission from a system driven by an arbitrary state of quantum light

Here we develop a general theory of the interaction between strong non-perturbative quantum light and a bound electron, i.e. atom. As shown previously (e.g., [1]), this approach can also describe the phase-matched HHG from many emitters, as in HHG from a strongly-driven gas. We can write a general Schrodinger equation for the joint density matrix of light and electron [2]:

$$i\hbar \frac{\partial \rho_0(t)}{\partial t} = \left[\hat{H}, \rho_0(t)\right], \tag{I. 1}$$

where the Hamiltonian is:

$$\hat{H} = \hat{H}_{\mathrm{A}} + \hat{H}_{\mathrm{F}} + \hat{\boldsymbol{d}} \cdot \hat{\boldsymbol{E}}. \tag{I. 2}$$

$\hat{H}_{\mathrm{F}} = \sum_{k\sigma} \hbar\omega\, \hat{a}_{k\sigma}^{\dagger}\hat{a}_{k\sigma}$ is the Hamiltonian of the electromagnetic field and $\hat{H}_A = \frac{\hat{\boldsymbol{p}}^2}{2m} + U(\boldsymbol{r})$ is the Hamiltonian of the bound electron. $\boldsymbol{k}$ is the wavevector that satisfies $\omega = c|\boldsymbol{k}|$, $\hat{\boldsymbol{p}}$ is the operator of the electron's momentum, m is the mass of the electron, $U(\boldsymbol{r})$ is the static potential of the bound electron, and $\hat{\boldsymbol{d}} = e\hat{\boldsymbol{r}}$ is the dipole moment of the bound electron. $\hat{\boldsymbol{E}} = i\sum_{\boldsymbol{k},\sigma} \epsilon^{(1)}\, \boldsymbol{\varepsilon}_{k\sigma}\left(\hat{a}_{k\sigma} - \hat{a}_{k\sigma}^{\dagger}\right)$ is a quantized electric field at the point $\boldsymbol{r} = \boldsymbol{0}$, with $\boldsymbol{\varepsilon}_{k\sigma}$ being the unit vector of the polarization. We define the quantized single-photon amplitude as $\epsilon^{(1)} = \sqrt{\frac{\hbar\omega}{2V\varepsilon_0}}$ [3]. We aim to solve this equation to describe the emission of an electron in an external electromagnetic field $\hat{\boldsymbol{E}}$ and static potential U. Henceforth, we use the term "atom" to refer to the bound electron system, while keeping in mind that the results are general.

We employ the interaction picture $\rho_0(t) \to e^{-\frac{i\hat{H}_F}{\hbar}t}\rho_0(t)e^{\frac{i\hat{H}_F}{\hbar}t}$, to obtain the following Schrodinger equation:

$$i\hbar\frac{\partial\rho_0(t)}{\partial t} = \left[\hat{H}_0(t), \rho_0(t)\right], \tag{I.3}$$

where $\hat{H}_0(t) = \hat{H}_A + \boldsymbol{d}\cdot\hat{\boldsymbol{E}}(t)$ and $\hat{\boldsymbol{E}}(t) = e^{-\frac{i\hat{H}_F}{\hbar}t}\hat{\boldsymbol{E}}e^{\frac{i\hat{H}_F}{\hbar}t} = i\sum_{\boldsymbol{k},\sigma}\epsilon^{(1)}\,\boldsymbol{\varepsilon}_{\boldsymbol{k}\sigma}\left(\hat{a}_{\boldsymbol{k}\sigma}e^{-i\omega_{k\sigma}t} - \hat{a}^{\dagger}_{\boldsymbol{k}\sigma}e^{i\omega_{k\sigma}t}\right)$.

Initially, before the action of the electromagnetic field on the atom, the field and the atom are not entangled and can be represented as a tensor product of light and atom density matrices: $\rho_0(0) = \rho_A(0)\otimes\rho_F(0)$. Moreover, for most experimental situations of interest, the atom is initially in its ground state, and therefore we take $\rho_A(0) = |g\rangle\langle g|$. The initial state of the field can be arbitrary. However, in the developments that follow, we consider that all the modes of the field $\boldsymbol{k}\sigma$ are in vacuum except driving field mode $\boldsymbol{k}_0\sigma_0$, which can be described with positive generalized P representation $P(\alpha,\beta^*)$ [4]:

$$\rho_F(0) = \int d^2\alpha_{\boldsymbol{k}_0\sigma_0}d^2\beta_{\boldsymbol{k}_0\sigma_0}\cdot P\left(\alpha_{\boldsymbol{k}_0\sigma_0},\beta^*_{\boldsymbol{k}_0\sigma_0}\right)\frac{|\alpha_{\boldsymbol{k}_0\sigma_0}\rangle\langle\beta_{\boldsymbol{k}_0\sigma_0}|}{\langle\beta_{\boldsymbol{k}_0\sigma_0}|\alpha_{\boldsymbol{k}_0\sigma_0}\rangle}\otimes\prod_{(\boldsymbol{k}\sigma)\neq(\boldsymbol{k}_0\sigma_0)}|0_{\boldsymbol{k}\sigma}\rangle\langle 0_{\boldsymbol{k}\sigma}|\,. \tag{I.4}$$

We should note that coefficients $P\left(\alpha_{\boldsymbol{k}_0\sigma_0},\beta^*_{\boldsymbol{k}_0\sigma_0}\right)$ in Eq. (I.4) is time-independent since it represents only the initial state of the field $\rho_F(0)$ and does not describe the dynamics of the field. Furthermore, we should also note that the $P\left(\alpha_{\boldsymbol{k}_0\sigma_0},\beta^*_{\boldsymbol{k}_0\sigma_0}\right)$ is positive finite and is unique for any quantum state as it is shown in [4], [5]. Since the Schrodinger equation Eq. (I.3) is linear, and $P\left(\alpha_{\boldsymbol{k}_0\sigma_0},\beta^*_{\boldsymbol{k}_0\sigma_0}\right)$ is time-independent, the solution can be written in form:

$$\rho_0(t) = \int d^2\alpha_{\boldsymbol{k}_0\sigma_0}d^2\beta_{\boldsymbol{k}_0\sigma_0}\cdot\frac{P\left(\alpha_{\boldsymbol{k}_0\sigma_0},\beta^*_{\boldsymbol{k}_0\sigma_0}\right)}{\langle\beta_{\boldsymbol{k}_0\sigma_0}|\alpha_{\boldsymbol{k}_0\sigma_0}\rangle}\rho_{\alpha\beta}(t), \tag{I.5}$$

where the elements $\rho_{\alpha\beta}(t)$ satisfy the following equation (substituting in Eq. (I.3)):

$$i\hbar\frac{\partial\rho_{\alpha\beta}(t)}{\partial t} = \left[\hat{H}_0(t), \rho_{\alpha\beta}(t)\right],$$

$$\rho_{\alpha\beta}(0) = |g\rangle\langle g|\otimes|\alpha_{\boldsymbol{k}_0\sigma_0}\rangle\langle\beta_{\boldsymbol{k}_0\sigma_0}|\otimes\prod_{(\boldsymbol{k}\sigma)\neq(\boldsymbol{k}_0\sigma_0)}|0_{\boldsymbol{k}\sigma}\rangle\langle 0_{\boldsymbol{k}\sigma}|.$$

Indeed, $\rho_{\alpha\beta}(t)$ is not Hermitian because it does not represent the density matrix but rather an intermediate step in the derivation. However, the total density matrix $\rho_0(t)$ is Hermitian. The solution of this equation can be formally written [6] as:

$$\rho_{\alpha\beta}(t) = U(t)\rho_{\alpha\beta}(0)U^{\dagger}(t), \tag{I.6}$$

$$U(t) = \hat{T}\exp\left(-\frac{i}{\hbar}\int_0^t d\tau\,\hat{H}_0(\tau)\right),$$

where $\hat{T}$ is time-ordering operator. The solution described by Eq. (I.6) is general and describes the system without any approximations.

We now employ coherent shift operators [3] with coherent parameters α and β (denoted by $D(\alpha)$ and $D(\beta)$) to define a new matrix element:

$$\tilde{\rho}_{\alpha\beta}(t) = D^{\dagger}\left(\alpha_{\boldsymbol{k}_0\sigma_0}\right)\rho_{\alpha\beta}(t)D\left(\beta_{\boldsymbol{k}_0\sigma_0}\right). \tag{I.7}$$

We substitute (I.6) into (I.7) and get:

$$\tilde{\rho}_{\alpha\beta}(t) = \left(D^{\dagger}\left(\alpha_{\boldsymbol{k}_0\sigma_0}\right)U(t)D\left(\alpha_{\boldsymbol{k}_0\sigma_0}\right)\right)|\mathrm{g}\rangle\langle\mathrm{g}| \otimes \prod_{(\boldsymbol{k}\sigma)}|0_{\boldsymbol{k}\sigma}\rangle\langle 0_{\boldsymbol{k}\sigma}|\left(D^{\dagger}\left(\beta_{\boldsymbol{k}_0\sigma_0}\right)U(t)D\left(\beta_{\boldsymbol{k}_0\sigma_0}\right)\right)^{\dagger}. \tag{I.8a}$$

By defining $|\Psi_{\alpha}(t)\rangle \equiv \left(D^{\dagger}\left(\alpha_{\boldsymbol{k}_0\sigma_0}\right)U(t)D\left(\alpha_{\boldsymbol{k}_0\sigma_0}\right)\right)|\mathrm{g}\rangle \otimes \prod_{(\boldsymbol{k}\sigma)}|0_{\boldsymbol{k}\sigma}\rangle$, we can rewrite Eq. (I.8) as:

$$\tilde{\rho}_{\alpha\beta}(t) = |\Psi_{\alpha}(t)\rangle\langle\Psi_{\beta}(t)|. \tag{I.8b}$$

The joint density matrix $\rho_0(t)$ then equals to:

$$\rho_0(t) \equiv \int d^2\alpha_{\boldsymbol{k}_0\sigma_0}d^2\beta_{\boldsymbol{k}_0\sigma_0} \cdot \frac{P\left(\alpha_{\boldsymbol{k}_0\sigma_0},\beta^*_{\boldsymbol{k}_0\sigma_0}\right)}{\langle\beta_{\boldsymbol{k}_0\sigma_0}|\alpha_{\boldsymbol{k}_0\sigma_0}\rangle}D\left(\alpha_{\boldsymbol{k}_0\sigma_0}\right)|\Psi_{\alpha}(t)\rangle\langle\Psi_{\beta}(t)|D^{\dagger}\left(\beta_{\boldsymbol{k}_0\sigma_0}\right). \tag{I.9}$$

Let's prove that this matrix has the correct norm for an arbitrary $P\left(\alpha_{\boldsymbol{k}_0\sigma_0},\beta^*_{\boldsymbol{k}_0\sigma_0}\right)$:

$$\mathrm{Tr}[\rho_0(t)] = \int d^2\alpha_{\boldsymbol{k}_0\sigma_0}d^2\beta_{\boldsymbol{k}_0\sigma_0} \cdot \frac{P\left(\alpha_{\boldsymbol{k}_0\sigma_0},\beta^*_{\boldsymbol{k}_0\sigma_0}\right)}{\langle\beta_{\boldsymbol{k}_0\sigma_0}|\alpha_{\boldsymbol{k}_0\sigma_0}\rangle}\langle\Psi_{\beta}(t)|D^{\dagger}\left(\beta_{\boldsymbol{k}_0\sigma_0}\right)D\left(\alpha_{\boldsymbol{k}_0\sigma_0}\right)|\Psi_{\alpha}(t)\rangle.$$

Now, we substitute the definition of $|\Psi_{\alpha}(t)\rangle$:

$$\mathrm{Tr}[\rho_0(t)] = \int d^2\alpha_{\boldsymbol{k}_0\sigma_0}d^2\beta_{\boldsymbol{k}_0\sigma_0} \cdot \frac{P\left(\alpha_{\boldsymbol{k}_0\sigma_0},\beta^*_{\boldsymbol{k}_0\sigma_0}\right)}{\langle\beta_{\boldsymbol{k}_0\sigma_0}|\alpha_{\boldsymbol{k}_0\sigma_0}\rangle} \times$$

$$\times \prod_{(\boldsymbol{k}\sigma)}\langle 0_{\boldsymbol{k}\sigma}|\,\langle\mathrm{g}|\left(D^{\dagger}\left(\beta_{\boldsymbol{k}_0\sigma_0}\right)U^{\dagger}(t)D\left(\beta_{\boldsymbol{k}_0\sigma_0}\right)\right)D^{\dagger}\left(\beta_{\boldsymbol{k}_0\sigma_0}\right)D\left(\alpha_{\boldsymbol{k}_0\sigma_0}\right)\left(D^{\dagger}\left(\alpha_{\boldsymbol{k}_0\sigma_0}\right)U(t)D\left(\alpha_{\boldsymbol{k}_0\sigma_0}\right)\right)|\mathrm{g}\rangle\prod_{(\boldsymbol{k}\sigma)}|0_{\boldsymbol{k}\sigma}\rangle.$$

We can simplify this to

$$\mathrm{Tr}[\rho_0(t)] = \int d^2\alpha_{\boldsymbol{k}_0\sigma_0}d^2\beta_{\boldsymbol{k}_0\sigma_0} \cdot \frac{P\left(\alpha_{\boldsymbol{k}_0\sigma_0},\beta^*_{\boldsymbol{k}_0\sigma_0}\right)}{\langle\beta_{\boldsymbol{k}_0\sigma_0}|\alpha_{\boldsymbol{k}_0\sigma_0}\rangle} \cdot \langle\beta_{\boldsymbol{k}_0\sigma_0}|\langle\mathrm{g}|U^{\dagger}(t)U(t)|\mathrm{g}\rangle|\alpha_{\boldsymbol{k}_0\sigma_0}\rangle,$$

and finally get:

$$\mathrm{Tr}[\rho_0(t)] = \int d^2\alpha_{\boldsymbol{k}_0\sigma_0}d^2\beta_{\boldsymbol{k}_0\sigma_0} \cdot P\left(\alpha_{\boldsymbol{k}_0\sigma_0},\beta^*_{\boldsymbol{k}_0\sigma_0}\right) = 1. \tag{I.10}$$

This proves that the density matrix has a well-defined norm.

By the definition $\left|\Psi_{\alpha/\beta}(t)\right\rangle$ can be written as the solution of the following Schrodinger equation:

$$\begin{cases} i\hbar\dfrac{\partial|\Psi_\alpha(t)\rangle}{\partial t} = H_\alpha(t)|\Psi_\alpha(t)\rangle \\ i\hbar\dfrac{\partial\left|\Psi_\beta(t)\right\rangle}{\partial t} = H_\beta(t)\left|\Psi_\beta(t)\right\rangle \end{cases}, \tag{I.11}$$

where $\left|\Psi_{\alpha/\beta}(0)\right\rangle = |\mathrm{g}\rangle \otimes \prod_{(\boldsymbol{k}\sigma)}|0_{\boldsymbol{k}\sigma}\rangle$ and

$$H_\alpha(t) = \hat{H}_\mathrm{A} + \hat{\boldsymbol{d}}\cdot\boldsymbol{E}_{\boldsymbol{\alpha}}(t) + \hat{\boldsymbol{d}}\cdot\hat{\boldsymbol{E}}(t), \qquad H_\beta(t) = \hat{H}_\mathrm{A} + \hat{\boldsymbol{d}}\cdot\boldsymbol{E}_{\boldsymbol{\beta}}(t) + \hat{\boldsymbol{d}}\cdot\hat{\boldsymbol{E}}(t),$$

and the classical fields are $\boldsymbol{E}_\alpha(t) = \langle\alpha|\hat{\boldsymbol{E}}|\alpha\rangle, \boldsymbol{E}_\beta(t) = \langle\beta|\hat{\boldsymbol{E}}|\beta\rangle$. Eq. (I.9) is exactly the equation describing HHG driven by a coherent light state $|\alpha\rangle$, which were considered in details in [1], [7]. Under the same assumptions as in these papers the solution is a product of coherent states:

$$\left|\Psi_{\alpha/\beta}(t)\right\rangle = \left|\phi_{\alpha/\beta}(t)\right\rangle \otimes \prod_{(\boldsymbol{k},\sigma)}\left|\gamma_{\boldsymbol{k}\sigma}^{\alpha/\beta}\right\rangle, \tag{I.12}$$

$$\gamma_{\omega\sigma}^{\alpha/\beta} = -\frac{i}{\hbar}\epsilon^{(1)}\boldsymbol{d}_{\alpha/\beta}(\omega)\cdot\boldsymbol{e}_\sigma, \qquad \boldsymbol{d}_{\alpha/\beta}(\omega) = \int_{-\infty}^{t} e^{i\omega\tau}\left\langle\phi_{\alpha/\beta}(\tau)\middle|\hat{\boldsymbol{d}}\middle|\phi_{\alpha/\beta}(\tau)\right\rangle d\tau.$$

In Eq. (I.10), the atomic state $\left|\phi_{\alpha/\beta}(t)\right\rangle$ is the solution of time-dependent Schrodinger equation (TDSE):

$$i\hbar\frac{\partial\left|\phi_{\alpha/\beta}(t)\right\rangle}{\partial t} = \left(\hat{H}_\mathrm{A} + \hat{\boldsymbol{d}}\cdot\boldsymbol{E}_{\boldsymbol{\alpha}/\boldsymbol{\beta}}(t)\right)\left|\phi_{\alpha/\beta}(t)\right\rangle. \tag{I.13}$$

Then, the exact solution of Eq. (I.1) for HHG driven by an arbitrary light state, is given by:

$$\rho_0(t) = \int d^2\alpha_{\boldsymbol{k}_0\sigma_0} d^2\beta_{\boldsymbol{k}_0\sigma_0}\,\frac{P\left(\alpha_{\boldsymbol{k}_0\sigma_0}, \beta^*_{\boldsymbol{k}_0\sigma_0}\right)}{\left\langle\beta_{\boldsymbol{k}_0\sigma_0}\middle|\alpha_{\boldsymbol{k}_0\sigma_0}\right\rangle}|\phi_\alpha(t)\rangle\langle\phi_\beta(t)| \times$$

$$\times\left(D\left(\alpha_{\boldsymbol{k}_0\sigma_0}\right)\prod_{(\boldsymbol{k}_1\sigma_1),(\boldsymbol{k}_2\sigma_2)}\left|\gamma_{\boldsymbol{k}_1\sigma_1}^{\alpha}\right\rangle\left\langle\gamma_{\boldsymbol{k}_2\sigma_2}^{\beta}\right| D^\dagger\left(\beta_{\boldsymbol{k}_0\sigma_0}\right)\right). \tag{I.14}$$

Limit of small single-photon field amplitude

Here we further consider the limit of $\epsilon^{(1)} \to 0$ (equivalent to $V \to \infty$), which holds in all current HHG experiments. Furthermore, Eq. (I.14) gives the joint density matrix of light and atom. We trace out the driving field mode $(\boldsymbol{k_0}, \sigma_0)$:

$$\rho(t) = \mathrm{Tr}_{\boldsymbol{k_0}\sigma_0}\left(\rho_0(t)\right).$$

We can simplify Eq. (I.15) and get:

$$\rho(t) = \int d^2\alpha_{\boldsymbol{k}_0\sigma_0} d^2\beta_{\boldsymbol{k}_0\sigma_0}\,P\left(\alpha_{\boldsymbol{k}_0\sigma_0}, \beta^*_{\boldsymbol{k}_0\sigma_0}\right)|\phi_\alpha(t)\rangle\langle\phi_\beta(t)| \otimes$$

$$\otimes\left(\frac{\left\langle\gamma^{\beta}_{\boldsymbol{k}_0\sigma_0}\middle|D^{\dagger}(\beta_{\boldsymbol{k}_0\sigma_0})D(\alpha_{\boldsymbol{k}_0\sigma_0})\middle|\gamma^{\alpha}_{\boldsymbol{k}_0\sigma_0}\right\rangle}{\langle\beta_{\boldsymbol{k}_0\sigma_0}|\alpha_{\boldsymbol{k}_0\sigma_0}\rangle}\right)\prod_{(\boldsymbol{k}_1\sigma_1),(\boldsymbol{k}_2\sigma_2)\neq(\boldsymbol{k}_0\sigma_0)}\left|\gamma^{\alpha}_{\boldsymbol{k}_1\sigma_1}\right\rangle\left\langle\gamma^{\beta}_{\boldsymbol{k}_2\sigma_2}\right|. \tag{I.15}$$

For an arbitrary single-mode light state, the generalized Glauber representation can be defined through the Husimi function Q [4]:

$$P(\alpha,\beta^*)=\frac{1}{4\pi}\exp\left(-\frac{|\alpha-\beta^*|^2}{4}\right)Q\left(\frac{\alpha+\beta^*}{2}\right).$$

Eq. (I.15) is written in terms of the coherent state amplitude α, which is related to the electric field:

$$E_{\alpha}(t)=i\epsilon^{(1)}\left(\alpha e^{-i\omega t}-\alpha^* e^{i\omega t}\right).$$

We introduce the complex amplitude of the field

$$\mathcal{E}_{\alpha}=2\epsilon^{(1)}\alpha, \tag{I.16}$$

and have the limit $\epsilon^{(1)}\to 0$ and $\alpha\to\infty$ in such a way that $\mathcal{E}_{\alpha}$ remains constant. Then we get:

$$P(\alpha,\beta^*)d^2\alpha\, d^2\beta=\lim_{\epsilon^{(1)}\to 0}\left(\frac{1}{4\pi}\frac{1}{4\left|\epsilon^{(1)}\right|^2}e^{-\frac{\left|\mathcal{E}_{\alpha}-\mathcal{E}_{\beta}\right|^2}{16\left|\epsilon^{(1)}\right|^2}}\right)Q\left(\frac{\alpha+\beta}{2}\right)d^2\alpha.$$

Considering that $Q\left(\frac{\alpha+\beta}{2}\right)$ is positive and its integral is unity, we can take the limit of $\epsilon^{(1)}\to 0$ separately for the exponent:

$$\lim_{\epsilon^{(1)}\to 0}\frac{1}{4\pi}\frac{1}{4\left|\epsilon^{(1)}\right|^2}e^{-\frac{\left|\mathcal{E}_{\alpha}-\mathcal{E}_{\beta}\right|^2}{16\left|\epsilon^{(1)}\right|^2}}=\delta^{(2)}\left(\mathcal{E}_{\alpha}-\mathcal{E}_{\beta}\right),$$

and get

$$\rho(t)=\int d^2\alpha\, Q(\alpha)|\phi_{\alpha}(t)\rangle\langle\phi_{\alpha}(t)|\otimes\prod_{(\boldsymbol{k}_1\sigma_1),(\boldsymbol{k}_2\sigma_2)\neq(\boldsymbol{k}_0\sigma_0)}\left|\gamma^{\alpha}_{\boldsymbol{k}_1\sigma_1}\right\rangle\left\langle\gamma^{\alpha}_{\boldsymbol{k}_2\sigma_2}\right|. \tag{I.17a}$$

Or in terms of electric field amplitudes:

$$\rho(t)=\int d^2\mathcal{E}_{\alpha}\cdot Q(\mathcal{E}_{\alpha})|\phi_{\alpha}(t)\rangle\langle\phi_{\alpha}(t)|\otimes\prod_{(\boldsymbol{k}_1\sigma_1),(\boldsymbol{k}_2\sigma_2)\neq(\boldsymbol{k}_0\sigma_0)}\left|\gamma^{\alpha}_{\boldsymbol{k}_1\sigma_1}\right\rangle\left\langle\gamma^{\alpha}_{\boldsymbol{k}_2\sigma_2}\right|. \tag{I.17b}$$

Eq. (I.17) gives the density matrix of the atom and light in all modes except for the drive $(\boldsymbol{k}_0\sigma_0)$. This density matrix is Hermitian, positively defined (because $Q(\alpha)$ is real positive) and has well-defined norm for an arbitrary state:

$$\mathrm{Tr}[\rho(t)]=\int d^2\mathcal{E}_{\alpha}\cdot Q(\mathcal{E}_{\alpha})\,\|\phi_{\alpha}(t)\|^2. \tag{I.18}$$

If we assume that the TDSE solution for atoms are normalized, i.e. $\|\phi_\alpha(t)\|^2 = 1$, then $\mathrm{Tr}[\rho(t)] = 1$.

We should note Eq. (I.17) just describes the total density matrix as the incoherent sum of solutions for the coherent states with probability described by $Q(\alpha)$. This happens because in the limit of $\epsilon^{(1)} \to 0$ and $\alpha \to \infty$, the two coherent states even with slightly different field amplitude $\mathcal{E}_\alpha$ are orthogonal, since $\alpha \to \infty$, $\beta \to \infty$ and thus $\langle \mathcal{E}_\alpha | \mathcal{E}_\beta \rangle \to 0$. We believe that this is the main reason of why only diagonal parts such as $|\alpha\rangle\langle\alpha|$ or equivalently $|\mathcal{E}_\alpha\rangle\langle\mathcal{E}_\alpha|$ are important.

We can also find the density matrix of the atom $\rho_{\mathrm{A}}(t)$:

$$\rho_{\mathrm{A}}(t) = \mathrm{Tr}_{\mathrm{F}}[\rho(t)] = \int d^2\alpha \cdot Q(\alpha) |\phi_\alpha(t)\rangle\langle\phi_\alpha(t)|\,, \tag{I.19a}$$

$$\rho_{\mathrm{A}}(t) = \mathrm{Tr}_{\mathrm{F}}[\rho(t)] = \int d^2\mathcal{E}_\alpha \cdot Q(\mathcal{E}_\alpha) |\phi_\alpha(t)\rangle\langle\phi_\alpha(t)|\,. \tag{I.19b}$$

The density matrix of the light $\rho_{\mathrm{F}}(t)$:

$$\rho_{\mathrm{F}}(t) = \mathrm{Tr}_{\mathrm{A}}[\rho(t)] = \int d^2\alpha \cdot Q(\alpha) \|\phi_\alpha(t)\|^2 \prod_{(\boldsymbol{k}_1\sigma_1),(\boldsymbol{k}_2\sigma_2)\neq(\boldsymbol{k}_0\sigma_0)} \left|\gamma^\alpha_{\boldsymbol{k}_1\sigma_1}\right\rangle \left\langle\gamma^\alpha_{\boldsymbol{k}_2\sigma_2}\right|, \tag{I.20a}$$

$$\rho_{\mathrm{F}}(t) = \mathrm{Tr}_{\mathrm{A}}[\rho(t)] = \int d^2\mathcal{E}_\alpha \cdot Q(\mathcal{E}_\alpha) \|\phi_\alpha(t)\|^2 \prod_{(\boldsymbol{k}_1\sigma_1),(\boldsymbol{k}_2\sigma_2)\neq(\boldsymbol{k}_0\sigma_0)} \left|\gamma^\alpha_{\boldsymbol{k}_1\sigma_1}\right\rangle \left\langle\gamma^\alpha_{\boldsymbol{k}_2\sigma_2}\right|. \tag{I.20b}$$

Energy, degrees of coherence and Mandel parameter of the emitted light

Now let's find the energy of the emitted light:

$$\varepsilon = \sum_{\boldsymbol{k}\sigma} \mathrm{Tr}\left(\rho_F(t=\infty) a^\dagger_{k\sigma} a_{k\sigma}\right) = \int d^2\alpha \cdot Q(\alpha) \|\phi_\alpha\|^2 \prod_{(\boldsymbol{k}_1\sigma_1)\neq(\boldsymbol{k}_0\sigma_0)} \left\langle\gamma^\alpha_{\boldsymbol{k}_1\sigma_1}\right| a^\dagger_{k\sigma} a_{k\sigma} \left|\gamma^\alpha_{\boldsymbol{k}_1\sigma_1}\right\rangle.$$

Using the properties of coherent states that $\left\langle\gamma^\alpha_{\boldsymbol{k}_1\sigma_1}\right| a^\dagger_{k\sigma} a_{k\sigma} \left|\gamma^\alpha_{\boldsymbol{k}_1\sigma_1}\right\rangle = |\gamma^\alpha_{k\sigma}|^2$, we get:

$$\varepsilon = \sum_{\boldsymbol{k},\sigma} \int \|\phi_\alpha\|^2 d^2\alpha\, Q(\alpha) |\gamma^\alpha_{k\sigma}|^2\,. \tag{I.21}$$

If now we substitute equation for $\gamma^\alpha_{k\sigma}$ and take into account that $\sum_{k\sigma} \ldots \to \frac{V}{(2\pi)^3 c^3} \int \omega^2 d\omega \sum_\sigma \int d\Omega \ldots$:

$$\frac{d\varepsilon}{d\omega} = \frac{\omega^4}{6\pi^2 \varepsilon_0 c^3} \int d^2\alpha\, Q(\alpha) \|\phi_\alpha\|^2 \cdot |\boldsymbol{d}_\alpha(\omega)|^2. \tag{I.22}$$

We also can find any degree of quantum coherence for each mode $g^{(n)}_{\boldsymbol{k}\sigma}$:

$$g^{(n)}_{\boldsymbol{k}\sigma} = \frac{\left\langle \left(a^\dagger_{k\sigma}\right)^n (a_{k\sigma})^n \right\rangle}{\left\langle a^\dagger_{k\sigma} a_{k\sigma} \right\rangle^n}. \tag{I.23}$$

Using the fact that $\left\langle\gamma^\alpha_{\boldsymbol{k}_1\sigma_1}\right| \left(a^\dagger_{k\sigma}\right)^n (a_{k\sigma})^n \left|\gamma^\alpha_{\boldsymbol{k}_1\sigma_1}\right\rangle = |\gamma^\alpha_{k\sigma}|^{2n} = \left|\epsilon^{(1)}\right|^{2n} |\boldsymbol{d}_\alpha(\omega) \cdot \boldsymbol{e}_\sigma|^{2n}$**.** We can substitute the density matrix $\rho_F(t)$ in Eq. (I.20) and we get:

$$g^{(n)}(\sigma,\omega)=\frac{\int d^2\alpha\, Q(\alpha)\|\phi_\alpha(t)\|^2|\boldsymbol{d}_\alpha(\omega)\cdot\boldsymbol{e}_\sigma|^{2n}}{(\int d^2\alpha\, Q(\alpha)\|\phi_\alpha(t)\|^2|\boldsymbol{d}_\alpha(\omega)\cdot\boldsymbol{e}_\sigma|^{2})^n}. \tag{I.24}$$

For example, Eq. (I.21) gives $g^{(n)}(\sigma,\omega)=1$ for the coherent state.

The special case of an extremely confined photonic mode

Let us consider emission into an optical mode with an extremely small interaction volume V (e.g., inside a cavity). We now calculate for which size of an interaction volume V, Eq. (I.17) does not work and more general Eq. (I.15) become necessary instead. The approximation of the previous section breaks down when:

$$\frac{|\mathcal{E}_\alpha|^2}{16\left|\epsilon^{(1)}\right|^2}=\frac{V\varepsilon_0|\mathcal{E}_\alpha|^2}{8\hbar\omega}=\frac{VI}{8c\hbar\omega}\sim 1. \tag{I.25}$$

For intensity $I=10^{14}$ W/cm^2 and wavelength $\lambda_0=800$ nm, we get $V=\frac{16\pi c^2\hbar}{I\lambda_0}\sim 10^{-27}$ m^3. Such an interaction volume corresponds to atomic-scale distances, currently below the range of even the strongest nanophotonic confinements [8]. Thus, Eq. (I.17) obtained in the limit of $\epsilon^{(1)}\to 0$ are correct for any realistic experimental scenario.

Husimi functions for different types of light

In this subsection, we show how to express the Husimi function Q as a function of the complex $\mathcal{E}_\alpha$ amplitude:

$$E_\alpha(t)=i/2\left(\mathcal{E}_\alpha e^{-i\omega t}-\mathcal{E}_\alpha^* e^{i\omega t}\right).$$

We can use this expression to simplify the Husimi functions in many important cases. The Husimi functions Q for coherent, Fock, thermal and BSV light states are taken from [3].

Coherent state light and Fock state light

$$Q_{\text{coherent}}(\alpha)d^2\alpha=\frac{1}{\pi}\exp(-|\alpha-\alpha_0|^2)\,d^2\alpha=\frac{\exp\left(-\frac{|\mathcal{E}_\alpha-\bar{\mathcal{E}}|^2}{4\left|\epsilon^{(1)}\right|^2}\right)}{4\left|\epsilon^{(1)}\right|^2\pi}d^2\mathcal{E}_\alpha, \tag{I.26}$$

$$Q_{\text{Fock}}(\alpha)=\frac{1}{\pi}\exp(-|\alpha|^2)\cdot\frac{|\alpha|^{2n}}{n!}=\frac{1}{\pi}\exp\left(-\left|\frac{|\mathcal{E}_\alpha|^2}{4\left|\epsilon^{(1)}\right|^2}\right|^2\right)\cdot\frac{|\mathcal{E}_\alpha|^{2n}}{\left(4\left|\epsilon^{(1)}\right|^2\right)^n n!}. \tag{I.27}$$

Both of these functions can be approximated as a delta-function in the limit $\epsilon^{(1)}\to 0$.

Thermal light

$$Q_{\text{thermal}}(\alpha)=\frac{1}{\pi(1+\bar{n})}\exp\left(-\frac{|\alpha|^2}{1+\bar{n}}\right). \tag{I.28}$$

In terms of the field amplitude, we have:

$$Q_{\text{thermal}}(\mathcal{E}_\alpha)d^2\mathcal{E}_\alpha = \frac{1}{\pi|\bar{\mathcal{E}}|^2}\exp\left(-\frac{|\mathcal{E}_\alpha|^2}{|\bar{\mathcal{E}}|^2}\right)d^2\mathcal{E}_\alpha. \quad \text{(I. 29)}$$

Bright squeezed vacuum (BSV)

$$Q_{\text{BSV}} = \frac{1}{\pi\cosh r}\exp\left(-\frac{2\alpha_y^2}{1+e^{2r}} - \frac{2\alpha_x^2}{1+e^{-2r}}\right). \quad \text{(I. 30)}$$

The average number of photons is: $\bar{n} = \sinh^2 r$. We assume that $\bar{n} \gg 1$: $\bar{n} \approx \frac{e^{2r}}{4}$

$$Q_{\text{BSV}} = \exp\left(-\frac{\alpha_y^2}{2\bar{n}} - \alpha_x^2\right) = \exp\left(-\frac{\alpha_y^2}{2\bar{n}}\right)\exp(-\alpha_x^2)\,. \quad \text{(I. 31)}$$

In terms of the field, we get:

$$Q_{\text{BSV}}(\mathcal{E}_\alpha) = \frac{1}{2|\bar{\mathcal{E}}|^2}\exp\left(-\frac{\text{Im}[\mathcal{E}_\alpha]^2}{2|\bar{\mathcal{E}}|^2}\right)\cdot\delta(\text{Re}[\mathcal{E}_\alpha]).$$

This result means that $\text{Re}[\mathcal{E}_\alpha]$ does not contribute to the ionization process if $r > 0$ and if we have a fixed phase for the BSV state. However, we know that for many implementations of BSV, especially in ultrashort pulses that may contain many modes, the phase varies and both options $r > 0$ and $r < 0$ alternate quickly during the same interaction [9]. In such situations, the light has a random phase. However, for the cut-off, it does not matter and we get the same result regardless of the phase:

$$Q_{\text{BSV}}(\mathcal{E}_\alpha) \approx \frac{1}{2\pi|\bar{\mathcal{E}}|^2}\exp\left(-\frac{|\mathcal{E}_\alpha|^2}{2|\bar{\mathcal{E}}|^2}\right). \quad \text{(I. 32)}$$

This phase-independence shows that the cut-off depends on the photon statistics of the driving light state and not on its entire quantum state.

II. Derivation of Cutoff Equations for Different States of Quantum Light

In the following section, we derive cutoff formulae for HHG driven by different quantum states of light. We begin by recalling the ponderomotive energy of a free electron interacting with a coherent state of light of electric field amplitude $\mathcal{E}$:

$$U = \frac{e^2|\mathcal{E}|^2}{4m\omega_0^2}. \tag{II. 1}$$

The probability for tunnel ionization of an atom by an electric field E is given by the ADK formula [10] and is denoted by $P_{\text{ion}}(E)$. Since the ponderomotive energy U is expressed in terms of the electric field ampletude $\mathcal{E}$, we can reformulate the $P_{\text{ion}}(\mathcal{E})$ in terms of the ponderomotive energy $U(\mathcal{E})$:

$$P_{\text{ion}}(U) \propto \left(\frac{1}{U}\right)^{\frac{1}{4I_p}-\frac{3}{4}} \exp\left(-\frac{2\sqrt{2}I_p^{3/2}}{3\omega_0 U^{1/2}}\right), \tag{II. 2}$$

where I_p is the ionization potential of the atom. We drop all non-exponential factors from this equation to approximate:

$$P_{\text{ion}}(U) \propto \exp\left(-a \cdot U^{-\frac{1}{2}}\right), \tag{II. 3}$$

where the parameter a is defined by $a = \frac{2\sqrt{2}I_p^{3/2}}{3\omega_0}$ and is not to be confused with the coherent state parameter α. Eq. (II.3) is plotted in Fig. II.1

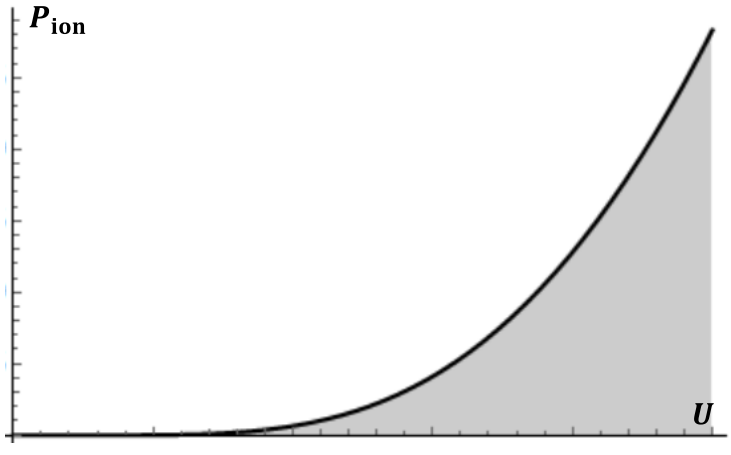

Fig. II.1: The probability for tunnel ionization of an atom P_{ion} as the function of the ponderomotive energy of an electron U.

For a quantum light state, the ponderomotive energy $U(\mathcal{E}_\alpha)$ and electric field amplitude $\mathcal{E}_\alpha$ (or coherent parameter α) are no longer definite numbers of the state. Rather, the electric field amplitude

exhibits fluctuations. Equivalently, the ponderomotive energy experiences corresponding fluctuations since it is a mathematical function of the field amplitude. The coherent parameter distribution of the quantum light state is given by the Husimi function $Q(\mathcal{E}_\alpha)$, where $\mathcal{E}_\alpha$ is a complex amplitude.

Each coherent state in the distribution $Q(\mathcal{E}_\alpha)$ results in different ponderomotive energy $U(\mathcal{E}_\alpha)$ and therefore, in a different ionization probability. The weighted probability that an electron undergoes tunnel ionization by a coherent component with ponderomotive energy $U(\mathcal{E}_\alpha)$ can be given by the product of the classical probability of ionization and Husimi function Q, which represents the fluctuation of the amplitude:

$$P_{\text{ion}}^{(\text{q})}(U) = \frac{1}{\text{norm}} P_{\text{ion}}^{(\text{c})}(U) Q(U). \tag{II. 4}$$

Husimi function for different types of light

In this subsection, we will express the Husimi function Q as the function of the ponderomotive energy U and the average ponderomotive energy $\overline{U}$. According to Eqs. (I.26-I.32) from section I, we get:

Coherent state light and Fock state light

$$Q_{\text{coherent}}(U) \approx Q_{\text{Fock}}(U) = \delta(U - \overline{U}). \tag{II. 5}$$

Thermal light

$$Q_{\text{thermal}}(\alpha) = \frac{1}{\overline{U}} \exp\left(-\frac{U}{\overline{U}}\right). \tag{II. 6}$$

Bright squeezed vacuum (BSV)

$$Q_{\text{BSV}}(U) = \frac{1}{2\overline{U}} \exp\left(-\frac{U}{2\overline{U}}\right). \tag{II. 7}$$

Therefore, BSV has a similar formula as thermal light, up to an additional coefficient of 2 in the exponent. Eqs. II.5-7 are shown in Fig. II.2a.

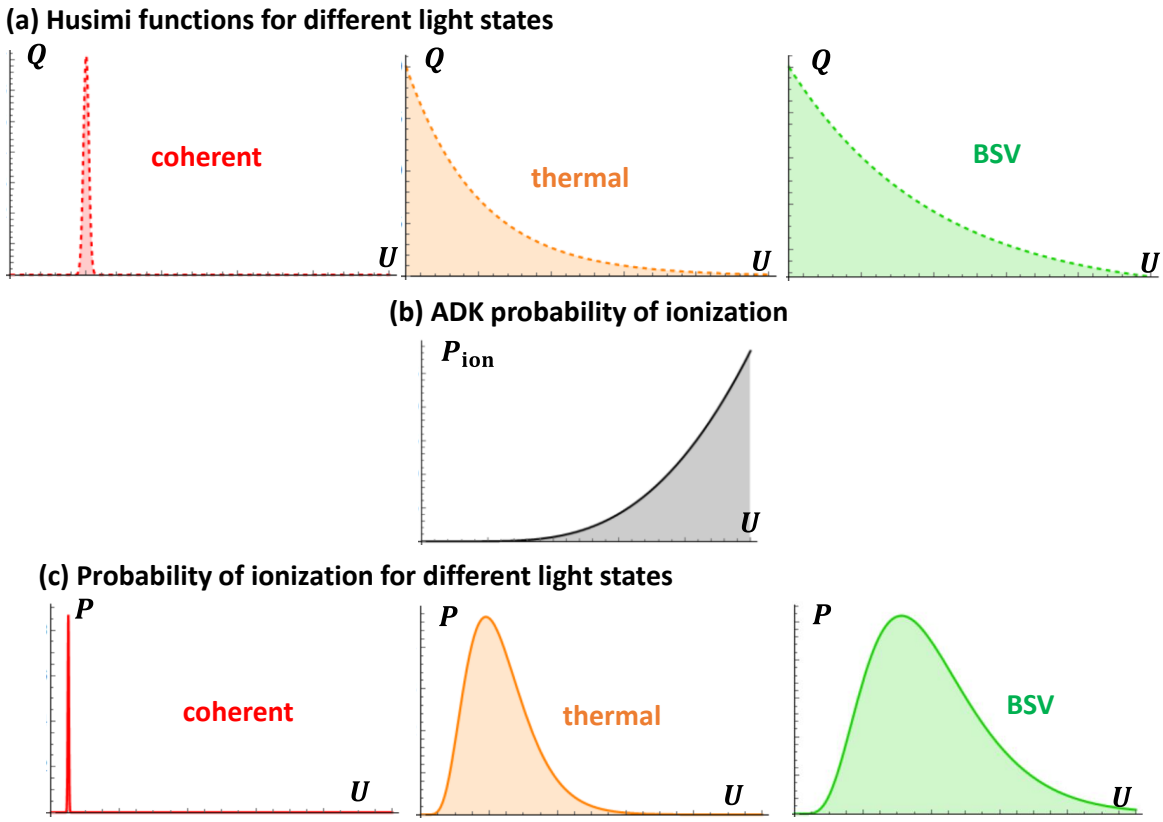

Fig. II.2: Interplay between the Husimi distribution and the ADK tunneling rate as the origin of the modified cutoff laws for quantum HHG. (a): Husimi distributions of electric field amplitudes (or alternatively intensities / ponderomotive energies) for the different quantum states of light. **(b)** The ADK tunneling rate as a function of the intensity of the driving *coherent* state field. **(c)** Weighted distribution for an electron to undergo tunnel ionization by a particular coherent component of the quantum state of light (written in terms of the ponderomotive energy). The bottom row is obtained by the multiplication of the top and middle rows.

Cutoff formulas for different states of light

We estimate the cutoff for an arbitrary quantum light state using the derivation of the conventional cutoff, and substituting the most probable field amplitude into the ponderomotive energy term $\bar{U} \to U_{\max}$:

$$E_{\text{cutoff}} = I_p + 3.17\, U_{\max}, \tag{II.8}$$

where $U_{\max}$ is the most probable amplitude so that:

$$\frac{dP(U)}{dU}\Big|_{U=U_{\max}} = 0.$$

Let us firstly consider the coherent and Fock states, for which the Husimi function is a delta-function:

$$P(U) \approx \frac{1}{\text{norm}} \exp\left(-a \cdot U^{-\frac{1}{2}}\right) \cdot \delta(U - \bar{U}). \tag{II.9}$$

To differentiate Eq. (II.9) we express the delta-function as a limit:

$$\delta(U-\bar{U}) = \lim_{\sigma\to 0}\frac{1}{\sigma\sqrt{\pi}}e^{-\frac{(U-\bar{U})^2}{\sigma^2}}$$

Thus, we have:

$$P(U) = \frac{1}{\text{norm}}\lim_{\sigma\to 0}\exp\left(-a\cdot U^{-\frac{1}{2}} - \frac{(U-\bar{U})^2}{\sigma^2}\right) \quad \text{(II. 10)}$$

The maximum of this equation satisfies $\frac{dP(U)}{dU} = 0$, providing $\sigma^2 a\cdot U_{\max}^{-3/2} - 4(U_{\max}-\bar{U}) = 0$. Then, in the limit $\sigma\to 0$ the solution is:

$$U_{\max} = \bar{U} + \frac{a\sigma^2}{4\bar{U}^{3/2}} + O(\sigma^4). \quad \text{(II. 11)}$$

Substituting a from Eq. (II.3) in Eq. (II.11), we get:

$$U_{\max} = \bar{U} + \frac{\sqrt{2}I_p^{3/2}}{6\omega_0\bar{U}^{3/2}}\cdot\sigma^2 + O(\sigma^4). \quad \text{(II. 12)}$$

Taking the limit $\sigma\to 0$ $U_{\max} = \bar{U}$ and we retrieve the conventional cutoff law: $I_p + 3.17\bar{U}$, as expected in the cases of coherent and Fock states. As we show below, the same derivation for the thermal and BSV states provide different cutoff laws (Fig. II.2c).

For a thermal and BSV states, we can write the probability function as:

$$P(U) = \frac{1}{\text{norm}}\exp\left(-a\cdot U^{-\frac{1}{2}} - \frac{U}{b\bar{U}}\right), \qquad b_{\text{BSV}} = 2, \qquad b_{\text{thermal}} = 1. \quad \text{(II. 13)}$$

We can find the mist probable amplitude $U_{\max}$ using:

$$\frac{d}{dU}\left(-a\cdot U^{-\frac{1}{2}} - \frac{U}{b\bar{U}}\right) = \frac{a}{2U_{\max}^{3/2}} - \frac{1}{b\bar{U}} = 0, \quad \text{(II. 14)}$$

$$U_{\max} = (a\cdot b\bar{U}/2)^{2/3}. \quad \text{(II. 15)}$$

Thus, for thermal and BSV, we have the following expressions for the cutoff respectively:

$$\text{cutoff of thermal state} = 1.92I_{\text{p}}(\bar{U}/\hbar\omega_0)^{2/3} + I_{\text{p}}. \quad \text{(II. 16)}$$

Similarly, we can derive the cutoff formula for the BSV state:

$$\text{cutoff of BSV state} = 3.05I_{\text{p}}(\bar{U}/\hbar\omega_0)^{2/3} + I_{\text{p}}. \quad \text{(II. 17)}$$

Summarizing these derivations, our approach provides further intuition for when the ponderomotive energy depends on the ionization potential: If the Husimi function $Q(\bar{U})$ has a sharp maximum (like for Fock and coherent states), then there is a term independent of the ionization potential. If the Husimi function $Q(\bar{U})$

does not have a sharp maximum (like for BSV and thermal states) then the ponderomotive energy may depend on the ionization potential. All the cutoffs are summarized in Table II.1 and are illustrated in Fig. II.3.

Table II.1. Analytical cutoff formulas for different quantum states of light

Coherent	$3.17 \cdot \bar{U} + I_p$
Fock	$3.17 \cdot \bar{U} + I_p$
Thermal	$1.92 I_p (\bar{U}/\hbar\omega_0)^{2/3} + I_p$
BSV	$3.05 I_p (\bar{U}/\hbar\omega_0)^{2/3} + I_p$

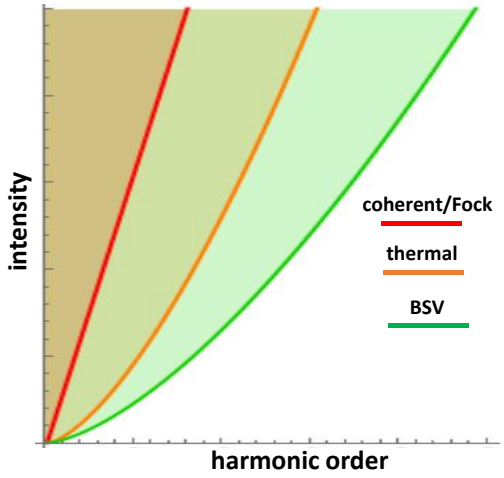

Figure II.3: Illustration of the cutoff laws for different states of driving light: Fock and coherent (red), thermal (orange), and bright squeezed vacuum (green).

It is important to note that even though the new cutoff laws contain an explicit ω_0, their scaling with ω_0 did not change compared to the conventional case (due to the additional implicit dependence inside $\bar{U}$):

$$\text{conventional cutoff} = 3.17\bar{U} + I_\text{p} = 3.17\frac{1}{\omega_0^2}\frac{e^2\langle E^2\rangle}{4m} + I_p\,,$$

$$\text{cutoff of BSV state} = 3.05 I_\text{p}(\bar{U}/\hbar\omega_0)^{2/3} + I_\text{p} = 3.05\frac{1}{\omega_0^2} I_\text{p}\left(\frac{e^2\langle E^2\rangle}{4m\hbar}\right)^{2/3} + I_\text{p}.$$

Let us also calculate the Mandel parameter Q_M of the considered quantum light states:

$$Q_\text{M} = \langle \Delta n^2\rangle/\langle n\rangle - 1.$$

Table II.2. The Mandel parameter of the considered quantum light states

Coherent	$Q_\text{M} = 0$
Fock	$Q_\text{M} = -1$
Thermal	$Q_\text{M} = \langle n\rangle$
BSV	$Q_\text{M} = 2\langle n\rangle + 1$

We see that the extended cutoff is observed for the super-Poissonian states.

III. Numerical calculation of the quantum optical HHG spectrum

In this section, we describe the numerical procedure employed for the calculation of the HHG spectrum generated by different quantum states of light. We consider a bound electron (i.e., an atom or another emitting system) driven by a quantum state of light with a generalized Glauber representation $P\left(\alpha_{\boldsymbol{k}_0\sigma_0}, \beta^*_{\boldsymbol{k}_0\sigma_0}\right)$and Husimi function $Q(\alpha)$. Explicit expressions for $P\left(\alpha_{\boldsymbol{k}_0\sigma_0}, \beta^*_{\boldsymbol{k}_0\sigma_0}\right)$ and $Q(\alpha)$ of different states are given below. We assume that at time $t = 0$, the atomic system occupies its ground state, which is denoted by $|\mathrm{g}\rangle$. Hence, the initial condition for the joint light-matter system is given by:

$$\begin{cases} \rho(0) = \rho_A(0) \otimes \rho_F(0) \\ \rho_A(0) = |\mathrm{g}\rangle\langle\mathrm{g}| \\ \rho_{\mathrm{F}}(0) = \int d^2\alpha_{\boldsymbol{k}_0\sigma_0} d^2\beta_{\boldsymbol{k}_0\sigma_0} \cdot P\left(\alpha_{\boldsymbol{k}_0\sigma_0}, \beta^*_{\boldsymbol{k}_0\sigma_0}\right) \dfrac{\left|\alpha_{\boldsymbol{k}_0\sigma_0}\right\rangle\left\langle\beta_{\boldsymbol{k}_0\sigma_0}\right|}{\left\langle\beta_{\boldsymbol{k}_0\sigma_0}\middle|\alpha_{\boldsymbol{k}_0\sigma_0}\right\rangle} \otimes \prod_{(\boldsymbol{k}\sigma)\neq(\boldsymbol{k}_0\sigma_0)} |0_{\boldsymbol{k}\sigma}\rangle\langle 0_{\boldsymbol{k}\sigma}| \end{cases}. \tag{III. 1}$$

Here $\left|\alpha_{\boldsymbol{k}_0\sigma_0}\right\rangle, \left|\beta_{\boldsymbol{k}_0\sigma_0}\right\rangle$ are coherent states with complex-valued coherent parameters $\alpha_{\boldsymbol{k}_0\sigma_0} = \alpha_x + i\alpha_y$, $\beta_{\boldsymbol{k}_0\sigma_0} = \beta_x + i\beta_y$, and $d^2\alpha_{\boldsymbol{k}_0\sigma_0} = d\alpha_x d\alpha_y, d^2\beta_{\boldsymbol{k}_0\sigma_0} = d\beta_x d\beta_y$. A quantum-optical coherent state $|\alpha\rangle$ corresponds to the emission of a laser, which is often approximated by a classical electromagnetic wave whose electric field is given by:

$$\boldsymbol{E}_\alpha(t) = i\epsilon^{(1)}\left(\alpha e^{-i\omega t} - \alpha^* e^{i\omega t}\right), \tag{III. 2}$$

where $\epsilon^{(1)}$ is known as the *single-photon amplitude* and is defined by $\epsilon^{(1)} = \sqrt{\hbar\omega/2V\epsilon_0}$. Here, ω is the frequency of the mode and V is the interaction volume. In effect, the complex-valued coherent parameter determines the amplitude and phase of a coherent state (also known as a *semi-classical state*).

We can calculate the spectrum of the emission using Eq. (I.22) which involves only $Q(\alpha)$ and is correct in the limit of $\epsilon^{(1)} \to 0$:

$$\frac{d\varepsilon}{d\omega} = \frac{\omega^4}{6\pi^2 c^3 \epsilon_0} \int d^2\alpha \|\phi_\alpha(t)\|^2 Q(\alpha) |\boldsymbol{d}_\alpha(\omega)|^2 . \tag{III. 3}$$

In the case of the equation with $Q(\alpha)$, we span the integrand in a 2-dimensional grid (α_x, α_y). Below, we construct the integrand using analytical formulae for $Q(\alpha)$.

Analytical formulas for $\boldsymbol{Q(\alpha)}$

$Q(\alpha)$ for a squeezed coherent state $|\gamma, r\rangle$ is given by [4]:

$$Q_{\mathrm{SC}}(\alpha) = \frac{1}{\pi\cosh(r)} \exp\left[-\frac{2\left(\alpha_y - \gamma_y\right)^2}{1 + e^{2r}} - \frac{2(\alpha_x - \gamma_x)^2}{1 + e^{-2r}}\right]. \tag{III. 6}$$

A coherent state is given by $|\gamma, 0\rangle$ and a squeezed vacuum state is given by $|0, r\rangle$. For the latter, $Q(\alpha)$ is given by [4]:

$$Q_{\mathrm{SV}}(\alpha) = \frac{\exp(-|\alpha|^2)}{\pi \cosh(r)} n! \exp\left[-\frac{1}{2}\tanh(r)\left(\alpha^2 + \alpha^{*2}\right)\right] \times$$

$$\times \left| \sum_{k=0} \left(\frac{\tanh(r)}{2}\right)^k \frac{(\alpha^*)^{n-2k}}{(n-2k)!\, k!} \times \left(\frac{1}{\cosh(r)}\right)^{n-2k} \right|^2 . \qquad \text{(III. 7)}$$

$Q(\alpha)$ for a squeezed thermal state (defined by r and by the average number of photons $\bar{n}$) is given by [4]:

$$Q_{\mathrm{ST}}(\alpha) = \frac{(\pi \bar{n} \cosh(r))^{-1}}{\left[\left(1 + \frac{1}{\bar{n}}\right)^2 - \tanh^2(r)\right]^{\frac{1}{2}}} \exp\left[-\frac{1}{2}\tanh(r)\left(\alpha^2 + \alpha^{*2}\right) - |\alpha|^2\right] \times$$

$$\times \exp\left[\frac{1/\cosh^2(r)}{(1 + 1/\bar{n})^2 - \tanh^2(r)}\left[\left(1 + \frac{1}{\bar{n}}\right)|\alpha|^2 - \frac{1}{2}\left(\alpha^2 + \alpha^{*2}\right)\tanh(r)\right]\right], \qquad \text{(III. 8)}$$

These different $Q(\alpha)$ functions (displayed in Fig. III.1) are used to calculate the spectra.

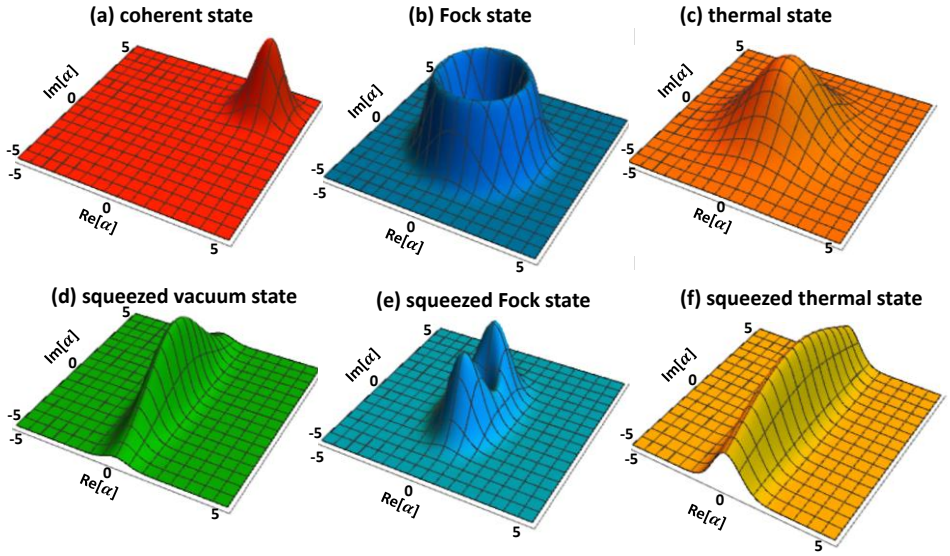

Fig. III.1: Husimi functions $Q(\alpha)$ for different states. (a) $Q(\alpha)$ for the coherent state, with $\gamma_x = \gamma_y = 3$; **(b)** $Q(\alpha)$ for Fock state with $n = 4$ photons; **(c)** $Q(\alpha)$ for the thermal state with the average number of photons $\bar{n} = 4$; **(d)** $Q(\alpha)$ for squeezed vacuum state with $r = 1.5$; **(e)-(f)** $Q(\alpha)$ for squeezed Fock and squeezed thermal states with $n = 1$ and $r = 0.5$.

Numerical calculation of the semi-classical dipole elements

The semi-classical dipole elements $d_\alpha(\omega)$ were obtained by numerically solving the time-dependent Schrodinger equation (TDSE) for an atom irradiated by a **classical** laser field $E_\alpha(t)$ as it is given in Eq. (III.2). The TDSE in atomic units within the dipole approximation is:

$$i\frac{\partial}{\partial t}\psi(t, x, y) = \left[-\frac{1}{2}\nabla^2 + V(r) + V_{ab}(r) + \boldsymbol{r} \cdot \boldsymbol{E}(\boldsymbol{r}, t)\right]\psi(t, x, y). \qquad \text{(III. 9)}$$

$\boldsymbol{E}(\boldsymbol{r},t)$ is the electric field and $V(r)$ is the atomic potential, modeled as a softened Coulomb potential [11]

$$V(r) = -\frac{1}{\sqrt{r^2 + a^2}}. \tag{III. 10}$$

The parameter a is set to $a = 0.8160$ bohr, to match the ionization potential of Ne, which is $I_p = 0.7924$ hartree [12]. $V_{ab}(r)$ is a complex absorbing potential, included in the equation to avoid nonphysical reflections of the wavefunction from the grid boundaries

$$V_{ab}(r) = \begin{cases} -i5 \times 10^{-4}(r - r_0)^3, & r \geq r0 \\ 0, & \text{otherwise} \end{cases} \tag{III. 11}$$

where $r_0 = 75$ bohr. The TDSE was solved by a 3rd order split-step method [13], [14], starting from the ground state of the model Ne atom. The ground state was found by representing field-free Hamiltonian in a matrix form on the cartesian spatial grid and diagonalizing it. The time-dependent propagation employed a trapezoid temporal envelope of the electric field, with 5-cycle long rise and fall sections and a 15-cycle long flat top section. The parameters of the pulse and the atomic potential are shown in Fig. III.2.

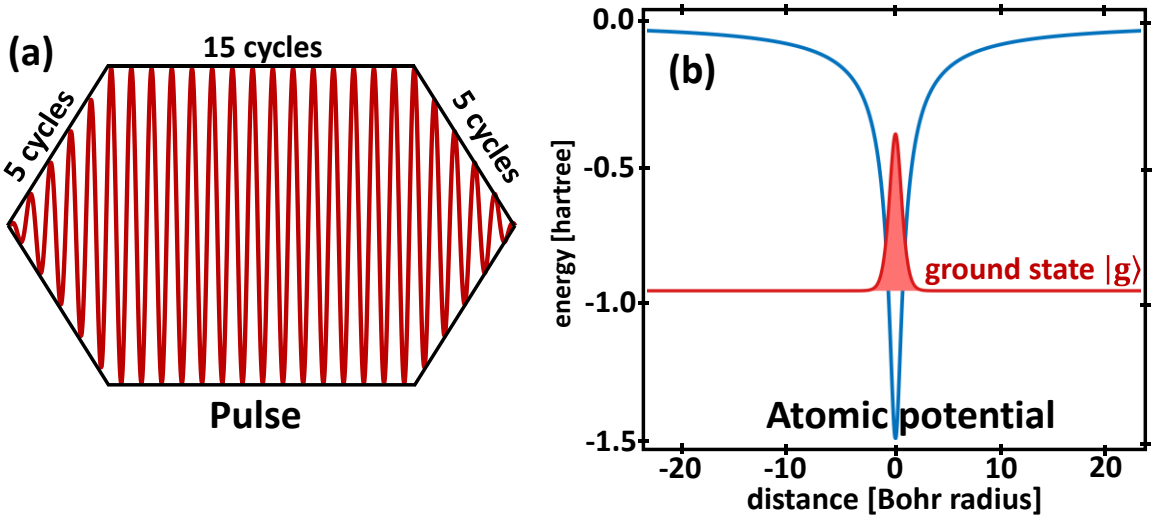

Fig. III.2: Characteristics of the driving field and of the atomic potential. (a) The time-dependent driving field has a trapezoid temporal envelope of the electric field, with 5-cycle-long rise and fall sections and a 15-cycle-long flat top section. **(b)** The atomic potential is modeled by $V(r) = -(r^2 + a^2)^{-1/2}$, with $a = 0.8160$ bohr, to match the Ne ionization potential, $I_p = 0.7924$ hartree [12].

Calculations were carried out on a 1D cartesian spatial grid, spanning from $x_{\min} = -100$ bohr to $x_{\max} = 100$ bohr, with a grid spacing of $dx = 0.06$ bohr and a timestep of $dt = 0.02$ a. u. The dipole acceleration was calculated by Ehrnfest's theorem:

$$\boldsymbol{a}(t) = -\langle \psi(\vec{r},t) | \boldsymbol{\nabla} V(r) + \boldsymbol{E}(t) | \psi(r,t) \rangle. \tag{III. 13}$$

From which, the harmonic spectra were obtained by a Fourier transform

$$\tilde{\boldsymbol{E}}(\omega) = \text{F. T.}\{\boldsymbol{a}(t)\}. \tag{III. 14}$$

Fig. III.3 presents the examples of HHG spectra numerically calculated using Eq. (III.14) for coherent, Fock, thermal, and BSV light for different intensities.

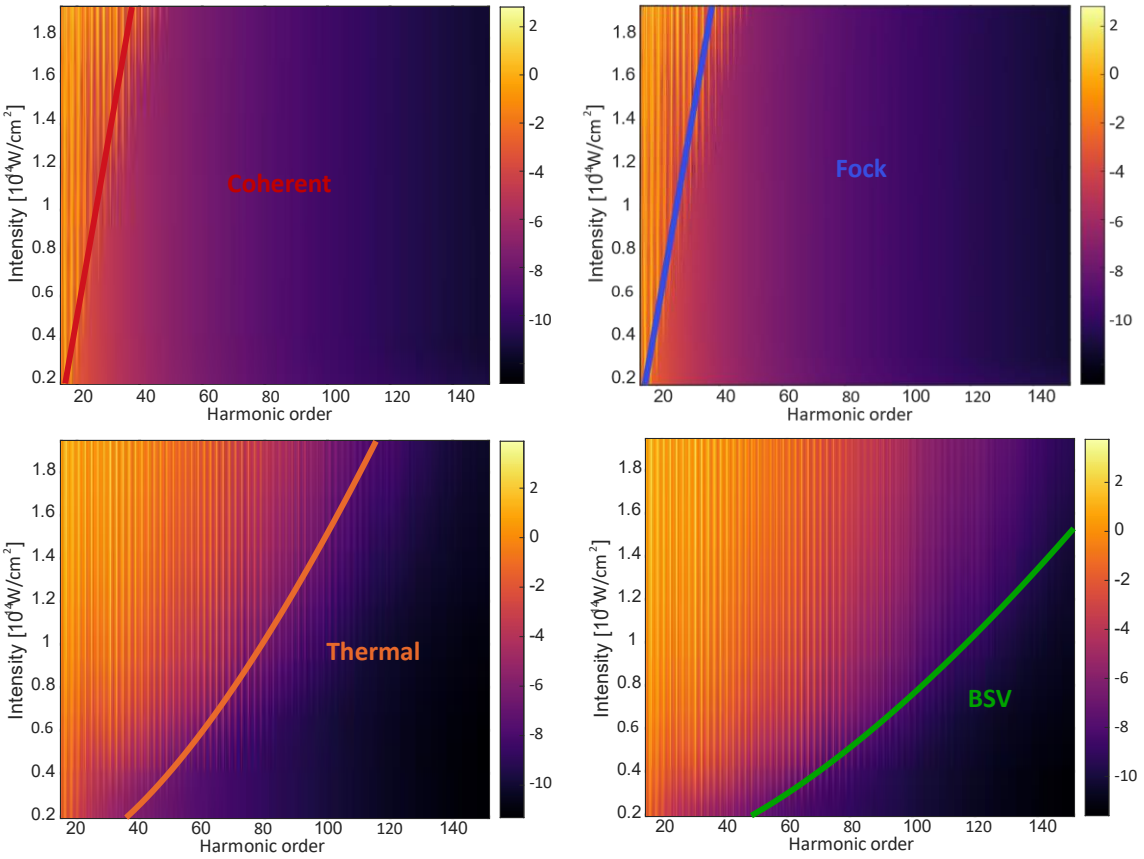

Fig. III.3: Maps of emission spectra for driving fields of different quantum states. The spectra for driving coherent, Fock, thermal, and BSV light states. Each color map shows the spectrum as a function of intensity (vertical) and frequency (horizontal). The intensity of the emission is shown by the color (log scale). The solid curves are the theoretical prediction of the cut-off for different quantum states. The theoretical model which explains these curves is presented in the next section. The wavelength of the driving field is λ_0 =800 nm.

We also calculate the total yield for each state of the driving field. The total yield is defined as the energy of the emitted light in all harmonics higher than the ionization potential $I_p/\hbar$:

$$\text{yield} = \int_{I_p/\hbar}^{\infty} \frac{d\varepsilon}{d\omega}\, d\omega,$$

where $d\varepsilon/d\omega$ is the spectrum of the emission calculated using Eq (I.22). The numerical results of the calculations are shown in Fig. III.4

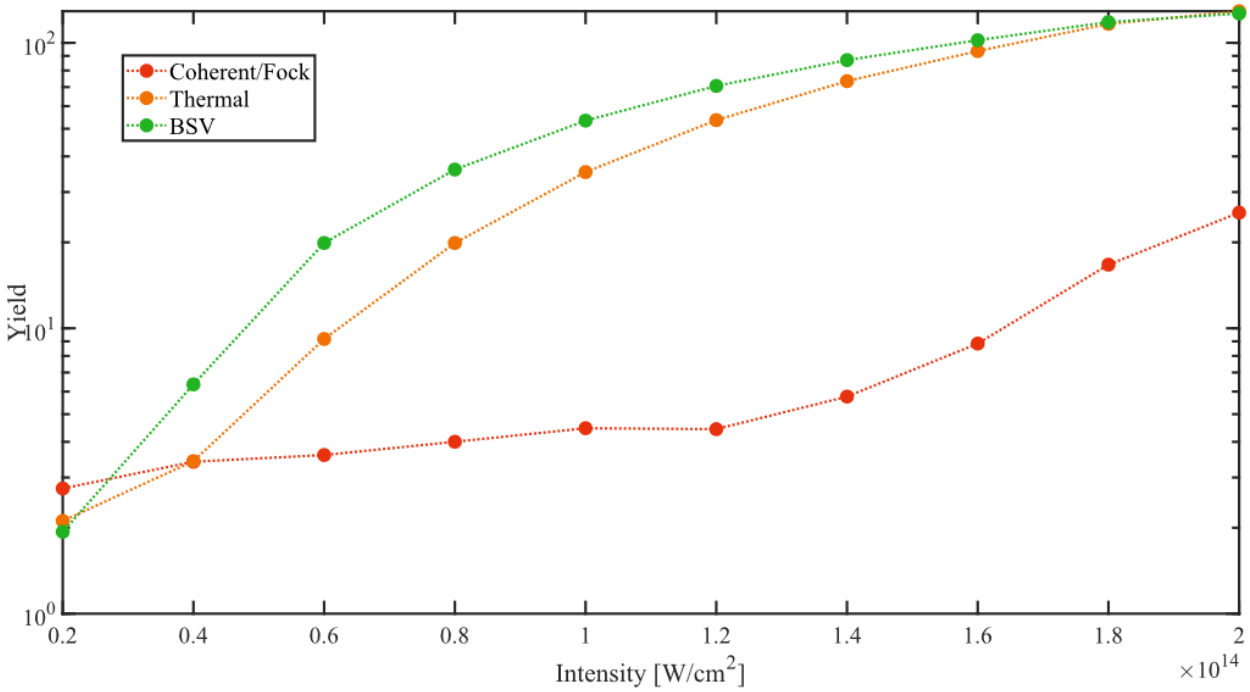

Fig. III.4: The total yield of the emission for driving fields of different quantum states. The total yield for driving coherent (Fock) thermal, and BSV light states. Coherent and Fock states, have the smallest total yield (red curve). Thermal and BSV light states have larger total yields and saturate faster (orange and green curves respectively). The yield is shown in a logarithmic scale. The wavelength of the driving field in all the calculations is λ_0 =800 nm.

BSV and thermal drivers have a larger yield than a coherent driver of the same intensity. The reason is exactly the same as for the extended cutoff: BSV and thermal light have extended Husimi distributions which leads to the strong fluctuations in the intensity and consequently higher yield.

IV. The threshold of BSV and thermal light intensity sufficient for the generation of HHG

In this section, we show that the intensity threshold for generating HHG driven by BSV is an order of magnitude less than for generating HHG driven by classical light (coherent state). The threshold can be defined by the intensity beyond which multiple pronounced high harmonic peaks appear above the background radiation. At the intensity threshold, these peaks start forming an approximated plateau.

Figure IV.1 shows two HHG spectra driven by classical light pulses of intensities (a) 10^{14} $\mathrm{W/cm^2}$ and (b) $2\times10^{14}\,\mathrm{W/cm^2}$. The latter intensity is above the threshold and generates multiple pronounced high harmonic peaks in the spectrum. This result is in agreement with previous experiments [15].

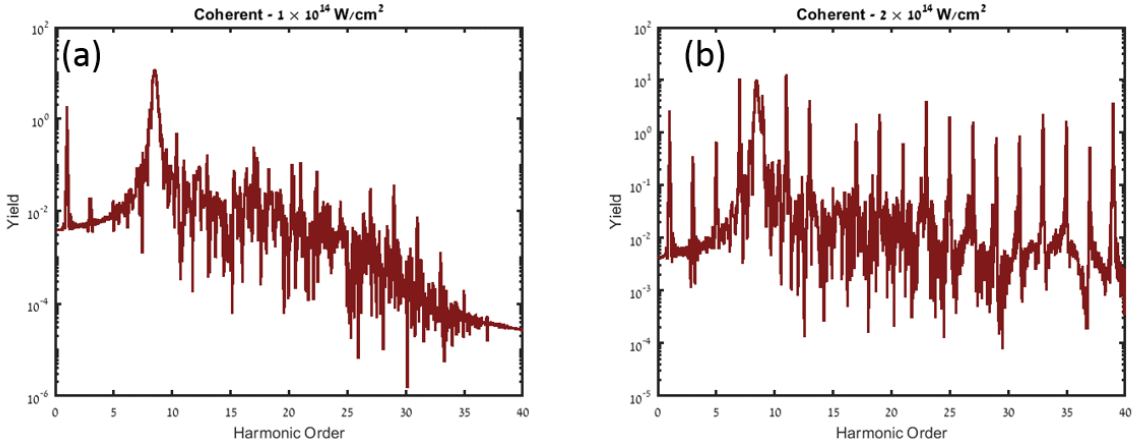

Fig. IV.1: The intensity threshold for the generation of HHG by classical light for a model Ne atom. (a,b) Comparison of the generated spectra for driver pulses of 1×10^{14} and $2\times10^{14}\,\mathrm{W/cm^2}$ peak intensities, showing the emergence of pronounced harmonics. The wavelength of the driving field is $\lambda_0 = 800$ nm.

Figure IV.2 shows two HHG spectra driven by bright squeezed vacuum pulses of intensities (a) 10^{13} $\mathrm{W/cm^2}$ and (b) $2\times10^{13}\,\mathrm{W/cm^2}$. The latter intensity is above the threshold and generates multiple well-pronounced high harmonic peaks in the spectrum. Note that this intensity is not sufficiency to generate HHG from classical light (as shown by the lack of high harmonic peaks in Figure IV.1a even for a higher intensity). Based on these simulations, we conclude that by driving HHG with BSV, instead of classical light, the intensity threshold is lowered by about an order of magnitude. We note that such BSV intensities were demonstrated in experiments [16] and thus show the feasibility of an experiment demonstrating HHG driven by BSV proposed in this work.

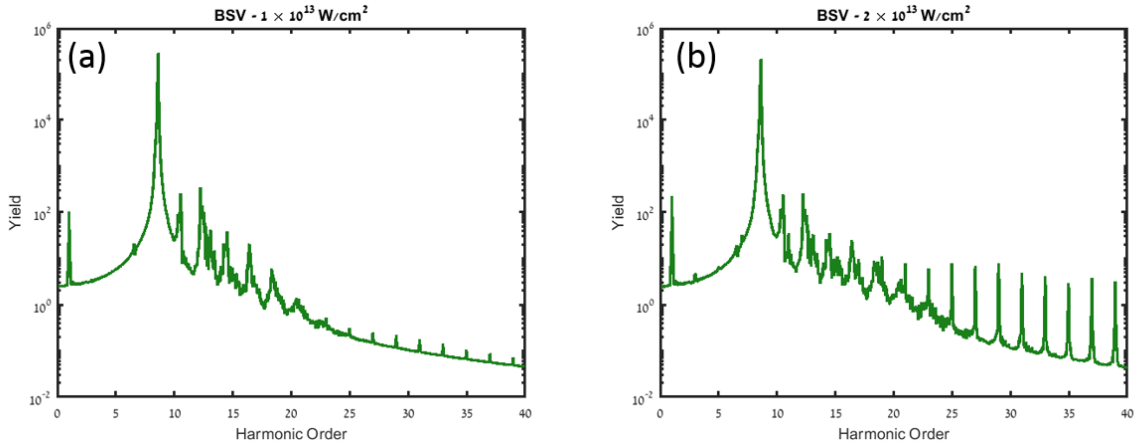

Fig. IV.2: The intensity threshold for the generation of HHG by BSV for a model Ne atom. (a,b) Comparison of the generated spectra for driver pulses of 1×10^{13} and 2×10^{13} W/cm^{2}peak intensities, showing the emergence of pronounced harmonics. The wavelength of the driving field is $\lambda_0 = 800$ nm.

We can estimate the number of generated harmonics for different light states using the cutoff laws in Eqs. (II.16, II.17). In all the numerical calculations, we used $I_p = 0.7924$ hartree. Let us assume that the non-perturbative regime and the HHG generation is when the cutoff is around 30$^{\text{th}}$ harmonic (Fig. IV.1a, Fig. IV 2a). Then, if we want to have 30 harmonics in the spectrum, we should drive the atom with the intensities written in the table.

Table IV.1. The needed drive intensities to generate 30 harmonics for each quantum light state

Coherent	$I = 1.3 \cdot 10^{14}$ W/cm^2
Fock	$I = 1.3 \cdot 10^{14}$ W/cm^2
Thermal	$I = 1.2 \cdot 10^{13}$ W/cm^2
BSV	$I = 0.7 \cdot 10^{13}$ W/cm^2

Importantly, a BSV driving field with such an intensity ($I = 0.7 \cdot 10^{13}$ W/cm^2) is experimentally feasible [16]. A thermal light state of intensity $I = 1.2 \cdot 10^{13}$ W/cm^2 is hard to generate but may be possible using random lasers [17]. A Fock state of intensity $I = 1.3 \cdot 10^{14}$ W/cm^2 is currently far beyond experimental reach.

References

[1] A. Gorlach, O. Neufeld, N. Rivera, O. Cohen, and I. Kaminer, "The quantum-optical nature of high harmonic generation," *Nat. Commun.*, vol. 11, no. 1, p. 4598, 2020, doi: 10.1038/s41467-020-18218-w.

[2] L. D. Landau and E. M. Lifshitz, *Quantum mechanics: non-relativistic theory*, vol. 3. Elsevier, 2013.

[3] M. O. Scully and M. S. Zubairy, "Quantum optics." American Association of Physics Teachers, 1999.

[4] M. S. Kim, F. A. M. De Oliveira, and P. L. Knight, "Properties of squeezed number states and squeezed thermal states," *Phys. Rev. A*, vol. 40, no. 5, pp. 2494–2503, 1989, doi: 10.1103/PhysRevA.40.2494.

[5] P. D. Drummond and C. W. Gardiner, “Generalised P-representations in quantum optics,” *J. Phys. A. Math. Gen.*, vol. 13, no. 7, p. 2353, 1980.

[6] A. Messiah, *Quantum Mechanics*. Dover Publications, 2014.

[7] M. Lewenstein *et al.*, “Generation of optical Schrödinger cat states in intense laser--matter interactions,” *Nat. Phys.*, vol. 17, no. 10, pp. 1104–1108, 2021.

[8] N. Rivera and I. Kaminer, “Light–matter interactions with photonic quasiparticles,” *Nat. Rev. Phys.*, vol. 2, no. 10, pp. 538–561, 2020, doi: 10.1038/s42254-020-0224-2.

[9] P. R. Sharapova *et al.*, “Properties of bright squeezed vacuum at increasing brightness,” *Phys. Rev. Res.*, vol. 2, no. 1, p. 13371, 2020.

[10] M. V Ammosov, “Tunnel ionization of complex atoms and of atomic ions in an altemating electromagnetic field,” *Sov. Phys. JETP*, vol. 64, p. 1191, 1987.

[11] L. Medišauskas, J. Wragg, H. Van Der Hart, and M. Y. Ivanov, “Generating Isolated Elliptically Polarized Attosecond Pulses Using Bichromatic Counterrotating Circularly Polarized Laser Fields,” *Phys. Rev. Lett.*, vol. 115, no. 15, p. 153001, 2015.

[12] O. Neufeld, A. Fleischer, and O. Cohen, “High-order harmonic generation of pulses with multiple timescales: selection rules, carrier envelope phase and cutoff energy,” *Mol. Phys.*, vol. 117, no. 15–16, pp. 1956–1963, Aug. 2019, doi: 10.1080/00268976.2018.1562126.

[13] J. A. Fleck, J. R. Morris, and M. D. Feit, “Time-dependent propagation of high-energy laser beams through the atmosphere,” *Appl. Phys.*, vol. 10, no. 1, p. 129, 1976, doi: 10.1007/BF00882638.

[14] M. D. Feit, J. A. Fleck Jr., and A. Steiger, “Solution of the Schrödinger Equation by a Spectral Method,” *J. Comput. Phys.*, vol. 47, pp. 412–433, 1982.

[15] O. H. Heckl *et al.*, “High harmonic generation in a gas-filled hollow-core photonic crystal fiber,” *Appl. Phys. B*, vol. 97, no. 2, pp. 369–373, 2009.

[16] T. S. Iskhakov, A. M. Pérez, K. Y. Spasibko, M. V Chekhova, and G. Leuchs, “Superbunched bright squeezed vacuum state,” *Opt. Lett.*, vol. 37, no. 11, pp. 1919–1921, 2012.

[17] G. Weng *et al.*, “Picosecond random lasing based on three-photon absorption in organometallic halide CH3NH3PbBr3 perovskite thin films,” *ACS Photonics*, vol. 5, no. 7, pp. 2951–2959, 2018.